



## Additive and subtractive modification of butterfly wing structural colors

Krisztián Kertész<sup>a,\*</sup>, Zsófia Baji<sup>a</sup>, András Deák<sup>a</sup>, Gábor Piszter<sup>a</sup>, Zsolt Rázga<sup>b</sup>, Zsolt Bálint<sup>c</sup>,  
László Péter Biró<sup>a</sup>

<sup>a</sup> Institute of Technical Physics and Materials Science, Centre for Energy Research, P.O. Box 49, H-1525 Budapest, Hungary

<sup>b</sup> University of Szeged, Department of Pathology, Dugonics tér 13, H-6720 Szeged, Hungary

<sup>c</sup> Hungarian Natural History Museum, 13 Baross St., H-1088 Budapest, Hungary

### ARTICLE INFO

#### Keywords:

Structural color  
Photonic crystal  
Butterfly wing, Langmuir-Blodgett  
ALD  
Oxygen plasma etching

### ABSTRACT

The modification of photonic nanoarchitectures occurring in butterfly wing scales with different nanostructures was investigated experimentally and by modeling. Single crystalline, polycrystalline, simple thin film, and pepper-pot-type photonic nanoarchitectures in the wing scales of different butterflies were investigated. By atomic layer deposition (ALD) (additive) the color of all nanoarchitectures was red shifted and by plasma etching (subtractive) the color of all nanoarchitectures was blue shifted in a controllable way. Langmuir-Blodgett multilayers of silica nanospheres were used as physical models. ALD produced color shifts similar to those for butterfly wings. In the case of a simple thin film, a theoretical calculation reproduced the spectral alterations well. For the more complex photonic nanoarchitectures, the general trends of the modifications were well reproduced by more sophisticated models, but differences in the magnitude of the alterations were found, attributed to the complex, random porous structures of the pepper-pot-type structures.

### 1. Introduction

Biological materials are made from a limited number of chemical elements (mainly C, H, O, S, P, N, and a few trace elements), with a wide variety of structural complexity [1–3]. Consequently, the structural properties of biological materials are exciting for materials scientists for replication [4], modeling [5], and devising potential applications [6]. Sub-micron structures are generated by diverse routes in nature; engineering methods using artificial materials can be used to construct similar structures [7,8]. It is useful to get a deeper insight into how the physical properties of these often sophisticated nanostructures of biological origin can be affected, by modifying their structural and material properties. An interesting example is of photonic nanoarchitectures, whose color can be tuned by external influences [9–13].

The use of ready-made complex 3D structures based on biological samples with the addition of a functional surface layer has been demonstrated for various purposes, such as for optical pH detection [14], gas and vapor detection [15,16], desorption-based vapor detection [17], high sensitivity SERS detection as a biotemplate [18,19], enhanced photocatalytic activity by tuning ZnO layer thickness [20], and for investigating the movement of muscle cells using the optical response signal of carbon nanotubes [11]. Oxygen plasma treatment can convert a

superhydrophobic surface [21,22] to a hydrophilic one [11]. Atomic layer deposition (ALD) can also change the surface properties [23]. ALD is an important method in materials science, as highly conformal layers can be grown at the molecular level, even with very large aspect ratios, leading to a variety of applications [24,25].

In the case of insects, functional nanostructures in the cuticle generate structural colors. These photonic nanoarchitectures exhibit highly diverse structures: from lamellar multilayer structures [26,27], through inverse opal-like [28], gyroid [29], and photonic amorphous [30] structures, many examples can be found. The nymphalid butterfly genus *Morpho* stands out as its optical properties have been particularly well explored, including the structure of its wing-scale nanoarchitectures [31,32]. Examples of replication and alteration of the nanostructures have been published, where the wing scales were used as biotemplates for sample preparation with variable reflectance [33]. Optical calculations have also been performed to determine structural colors [34–36], and, in the case of the species *Papilio blumei*, a TiO<sub>2</sub> ALD coating was used to tune the wing reflectance [37,38]. The wings of another *Morpho* species, *Morpho sulkowskyi*, were modified using oxygen plasma treatment, which etched the nanoarchitecture, resulting in a shift of structural color [39].

Bioinspired nanoarchitectures, self-assembled with the Langmuir-

\* Corresponding author.

E-mail address: [kertesz@mfa.kfki.hu](mailto:kertesz@mfa.kfki.hu) (K. Kertész).

<https://doi.org/10.1016/j.colcom.2020.100346>

Received 7 September 2020; Received in revised form 17 November 2020; Accepted 19 November 2020

Available online 8 December 2020

2215-0382/© 2020 The Authors.

Published by Elsevier B.V. This is an open access article under the CC BY-NC-ND license

(<http://creativecommons.org/licenses/by-nc-nd/4.0/>).

Blodgett (L-B) technique [40,41] from monodisperse silica nanospheres with an appropriate diameter, can produce a series of photonic structures with diverse colors in the visible and infra-red ranges [41]. They can be used as less complex comparison samples to better understand the changes induced by a given treatment in the properties of photonic nanoarchitectures of biological origin.

In this work, controlled modifications were performed on photonic nanoarchitectures of structurally colored butterfly wings: of biological origin, built mainly from chitinous materials; and of bioinspired samples fabricated using the L-B method. Two distinct methods were used, thinning by oxygen plasma treatment and thickening by ALD, to obtain a series of optically modified sample sets. Scanning and transmission electron micrographs were taken of the sample series thus obtained. The samples were subjected to optical spectrometry, and the results were compared to optical simulations. The two surface modification methods were found to be well suited for precisely changing the structural colors of photonic nanoarchitectures.

## 2. Materials and methods

Wing samples originated from three species representing the family of Gossamer-winged butterflies (Lycaenidae, Papilionoidea, Lepidoptera): Blue Harlequin (*Mimeresia neavei*), Common Blue (*Polyommatus icarus*), and Remus Greenstreak (*Cyanophrys remus*). The species *P. icarus* is a Transpalearctic species inhabiting open landscape areas. The species *C. remus* is Neotropical; the species *M. neavei* is Afrotropical; both live in forested regions. The specimens examined were provided by the Lepidoptera collection of the Hungarian Natural History Museum.

For the preparation of the mono- and multilayer Langmuir-Blodgett films, an approach was employed that we reported previously [42]. Briefly, Stöber silica nanoparticles with ca. 500 nm diameter were synthesized, suspended in ethanol, and mixed with chloroform in a 2:1 volume ratio. This was spread onto the water surface in a Langmuir trough. After evaporation of the solvent, the particles were compressed to form a close-packed monolayer as inferred from their surface pressure–area isotherms. Langmuir-Blodgett monolayers were prepared by vertical deposition of the interfacial films on 2-in. Si wafers. The monolayer formation and deposition process was repeated, resulting in multilayers consisting of 1, 2, 3, and 5 monolayers.

Pieces of butterfly wings and L-B samples were coated with 5, 10, 20, 30, and 40 nm thick  $\text{Al}_2\text{O}_3$  layers in a Picosun Sunale R-100 ALD reactor. A trimethyl-aluminum (TMA) precursor and water vapor as oxidant were used for the deposition of  $\text{Al}_2\text{O}_3$ . The TMA was electronic grade purity and purchased from Strem Chemicals. The deionized water was 17 M $\Omega$  purity. Both reagents were kept at room temperature. The carrier gas and purging medium was 99.999% purity nitrogen. Flow rates of the precursor gases and water were 150 sccm. During deposition, the pressure in the chamber was kept at 15 mbar. In order to coat these very high aspect ratio structures, longer pulsing times were needed so as to leave the precursors enough time to diffuse into the pores. Whereas 0.1 s long pulses and 3 s purging times are enough to saturate flat surfaces, the deposition cycles in this case were chosen as follows: the pulse lengths of the precursors were 0.5 s, and the purging times were 15 s after the TMA pulses, and 20 s after the water pulses. As the wing samples were thermally sensitive, the growth temperature was maintained at 100 °C.

For wing surface treatment, the Diener Zepto low pressure plasma system was used. Pieces of butterfly wings were cut of approximately 1 cm<sup>2</sup>, which were subjected to 1–5 min of oxygen plasma etching at 0.4 mbar. At the start of the experiments, the vacuum chamber was flushed a few times with oxygen.

Spectral characterization was done using Avantes modular fiber optic instruments in the UV-VIS-NIR range. An Avalight DH-S-BAL light source was used with an AvaSpec-HERO spectrophotometer and a 30 mm diameter integrating sphere was in contact with the samples for the reflectance measurements. The angle-dependent measurements were carried out using a home-made goniometric setup [43].

Optical micrographs of wing scales in reflected light were taken using a Zeiss Axio Imager A1 microscope with the attached digital AxioCam ICc 5 camera.

Samples of a few mm<sup>2</sup> were cut for scanning electron microscope (SEM) inspection. To avoid undesired surface modification, metallic coating to make the samples conductive was not applied. A Zeiss LEO 1540 XB SEM with careful parameter adjustment made it possible to obtain images without charging artifacts.

For transmission electron microscopy (TEM), butterfly wing pieces were wetted with acetone and embedded into EMBED812 (EMS) resin. Sections of 70 nm were produced by a Leica Ultracut S ultramicrotome. After staining with uranyl acetate and lead citrate, the sections were observed using a Philips CM10 TEM equipped with a digital camera, MegaView G2 and iTEM imaging analysis software by Olympus.

## 3. Results and discussion

The structural color of the butterfly wings in these investigations was determined by the characteristic sizes of the photonic nanostructures and the refractive indices of the materials building up the wing scales (chitin and air). First, color modification of different ordered 3D structures was examined, using the special case of the male butterfly *C. remus*, which has scales with different types of nanoarchitectures [43] on the two sides of its wings. Each side of the wings has two layers of scales. Cover scales form the upper layer, generating color from pigments and photonic nanoarchitectures. Ground scales form the layer closer to the wing membrane, containing melanin, a pigment with a broad absorption band in the UV-VIS. In its original state, the cover scales of the blue dorsal side contain a long-range ordered nanostructure, while on the ventral side there are micron-sized crystallites in different orientations resulting in differently colored domains [43] with peculiar light reflectance patterns originating from a well-ordered gyroid structure [44].

The wing was cut into multiple narrow pieces to obtain enough samples for the experiments, using their dorsal and ventral sides for plasma treatment and ALD. The lack of larger samples meant that reliable reflectance measurements were not possible. Thus optical micrographs were taken under the same illumination conditions, and focus stacking of the images was applied to enhance the depth of field. There was no other post-processing carried out, therefore the visible color shift observed in the images is free from any artifacts (Fig. 1). The micron-size domains (crystallites) on the ventral side cover scales kept their differences in color after treatment with both plasma etching and ALD, but their color was blue-shifted (plasma etching), or red-shifted (ALD). Both blue (dorsal wing side) and green (ventral wing side) samples followed the general trend of red-shifting due to the ALD treatment and blue-shifting due to the plasma etching (which was also observed for other samples possessing different nanostructures). The chemical coloration of the ground scales (indicated with red ovals in Fig. 1(a) and (f)) was found to be brown, regardless of the surface modification that was applied (Fig. 1(g), (h), (i), and (j)). The lack of change in coloration after the applied treatment clearly shows whether a wing scale is colored only by pigments (no color shift observed) or by pigments and photonic crystal structure (color shift observed).

A different, open structure – the so-called pepper-pot structure – is to be found in the wing scales of many male butterflies representing the Lycaenid family studied by our group [45]. This quasiordered structure is constituted of perforated layers of chitin, stacked in such a way that the interlayer distance is maintained by pillars of chitin. It has chitin-rich and air-rich layers. A typical example is the butterfly *P. icarus* [46]. Fig. 2(a) shows electron micrographs of a typical scale, where the spongy structure in the area between the ridges and the cross-ribs determines the blue color. Because it is a highly-permeable structure, the ALD precursors entered the deepest areas in the pores and resulted in conformal thickening of the chitin nanostructures. Fig. 2(c) shows a scale structure with a 40 nm ALD coating. The size of the holes determines how thick the ALD layer can be; in these experiments the

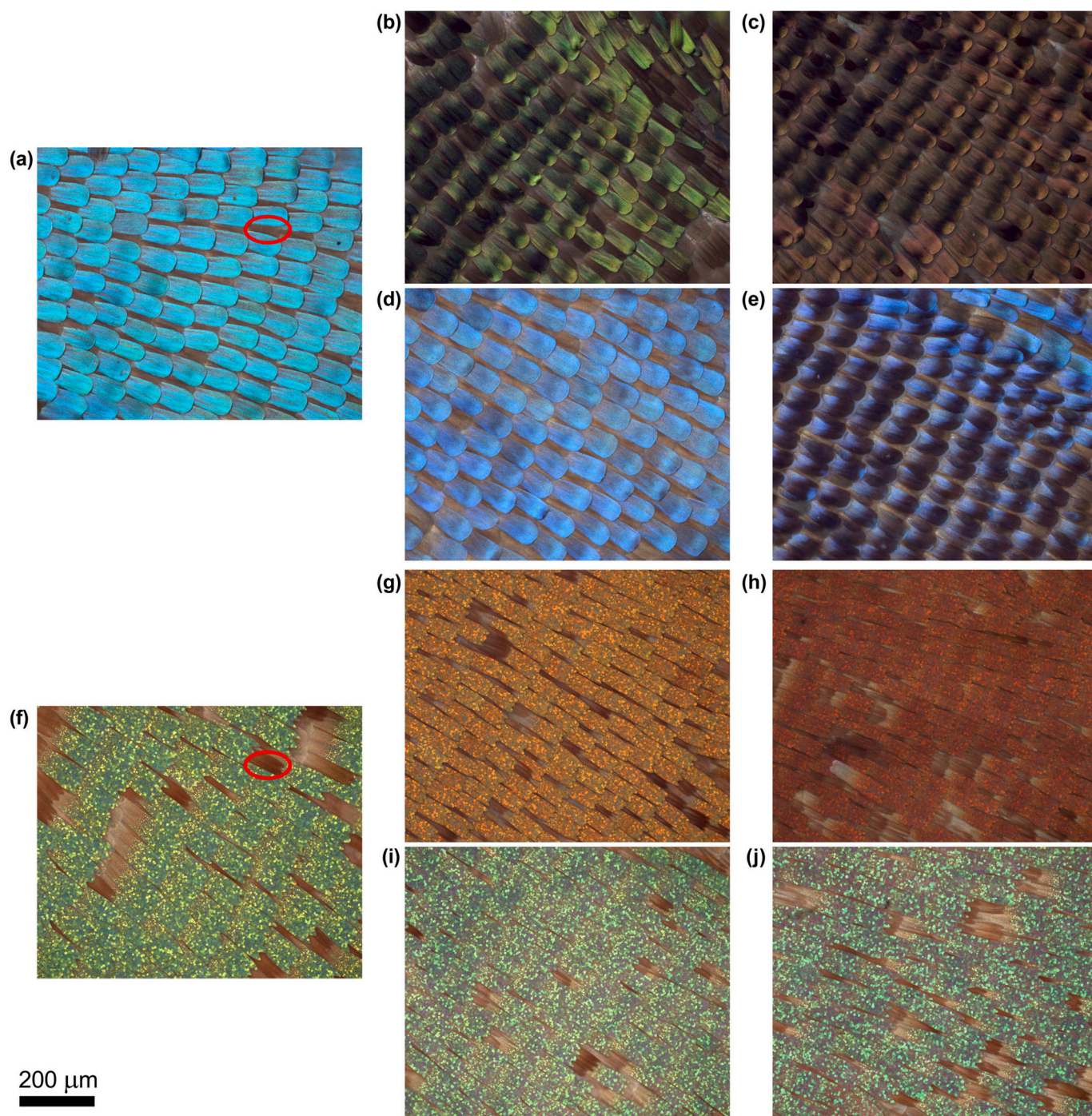


**Fig. 1.** Optical micrographs of *Cyanophrys remus* wings. (a) Pristine dorsal side; (b) dorsal side with 20 nm ALD and (c) dorsal side with 40 nm ALD; (d) dorsal side after 2 min of plasma treatment and (e) dorsal side after 4 min of plasma treatment; (f) pristine ventral side; (g) ventral side with 20 nm ALD and (h) ventral side with 40 nm ALD; (i) ventral side after 2 min of plasma treatment and (j) ventral side after 4 min of plasma treatment. On (a) and (f) the red ovals mark brown-pigmented ground scales below the layer of cover scales. (For interpretation of the references to color in this figure legend, the reader is referred to the web version of this article.)

intention was to avoid full closing of the pores. The result of the conformal coating process is revealed precisely by TEM imaging as shown in Fig. 2(d), where the outer  $\text{Al}_2\text{O}_3$  layer on the surface is darker than the chitin. The thickness can be measured more precisely than on the SEM images.

By contrast, oxygen plasma treatment erodes and thins the chitin: the ridges become narrower and the cross-ribs are hardly visible. In the pepper-pot region, the ratio of chitin to air voids is reversed, as can be seen in Fig. 2(b). This process has a limit, as after a certain level the

material completely disappears, the integrity of the structure vanishes, and the wing scale nanoarchitecture collapses. According to our experiments, after 8 min of thinning in oxygen plasma the layers in the scales were not preserved.

The change in the species-specific blue reflectance spectrum of *P. icarus* (Fig. 3) was measured by means of an integrating sphere as it is less sensitive to irregularities on the wing [46]. As with *C. remus*, ALD shifted the reflected spectrum from *P. icarus* wings towards longer wavelengths, while oxygen plasma treatment shifted reflections towards

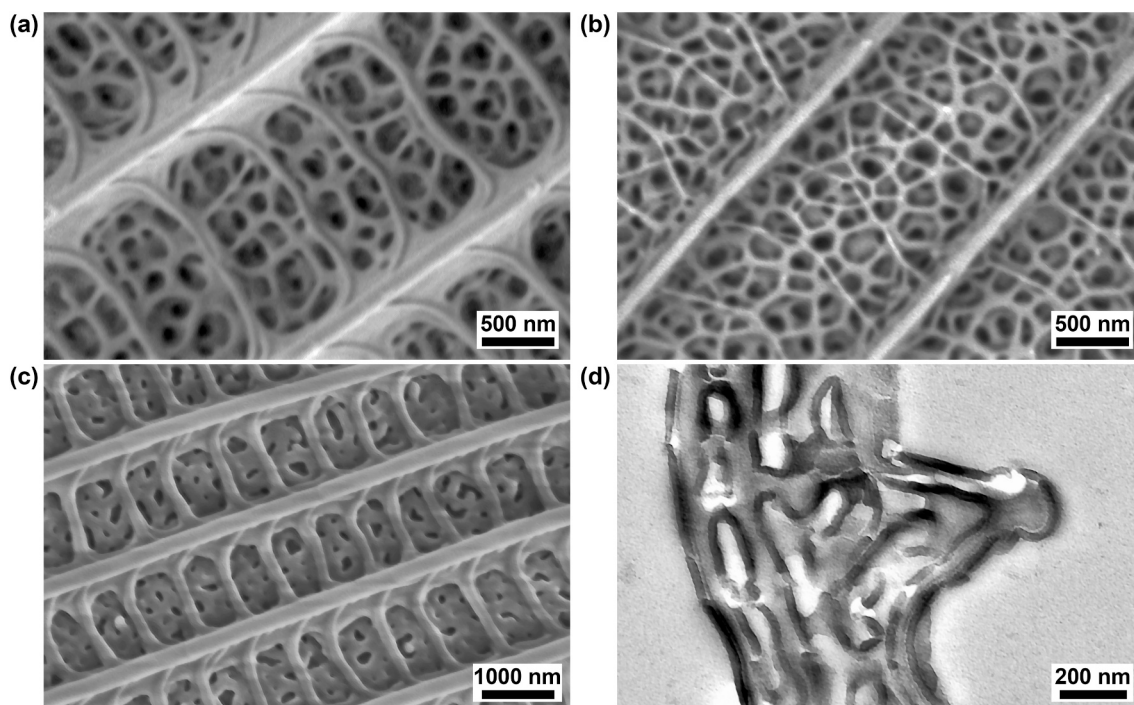


**Fig. 2.** Scanning and transmission electron micrographs of *Polyommatus icarus* cover scales on the dorsal wing surface. (a) Pristine; (b) after 2 min of oxygen plasma treatment; (c) with a 40 nm ALD layer of  $\text{Al}_2\text{O}_3$ ; (d) a TEM image of sample (c).

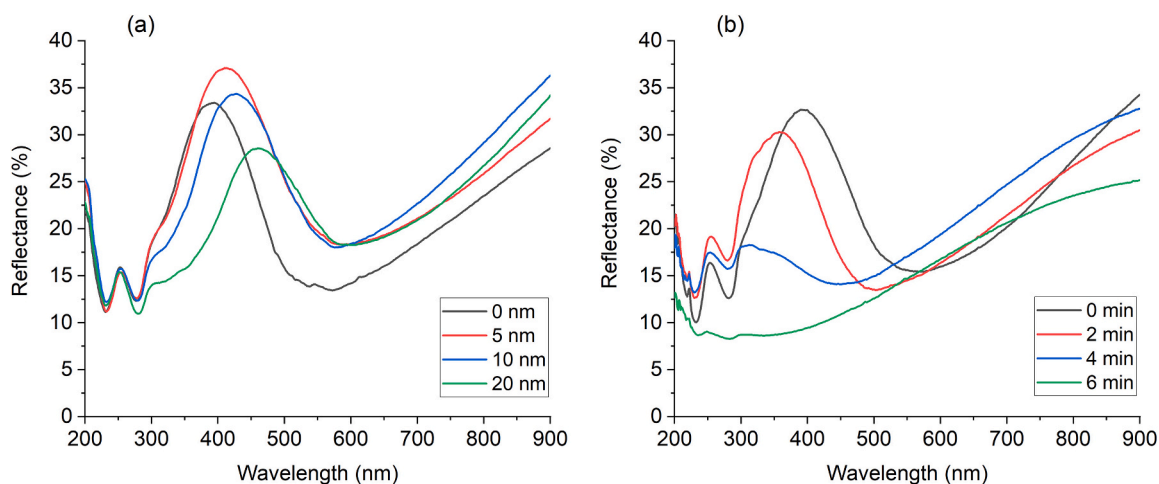


**Fig. 3.** Optical reflectance spectra measured with an integrating sphere on *Polyommatus icarus* wings. (a) With increasing thickness of deposited  $\text{Al}_2\text{O}_3$  layers, and (b) after oxygen plasma treatment of increasing durations.

shorter wavelengths. The magnitude of the shifts was beyond 70 nm. After 6 min of plasma treatment, the peak of the structural blue reflectance completely disappeared and the characteristic spectrum of unstructured pigmented (containing only melanin) brown scales was obtained. Whether from the thickening or thinning side, until the reflectance peak begins to collapse, these modifications can be used to precisely tune the reflectance of porous photonic structures made by both methods. As on porous 3D structures, the entire volume of the samples can be accessed, therefore the surface modification techniques have stronger effects on optical and chemical properties which may be a benefit in applications [10,16].

To investigate the color change on a controllably built and open structure similar to the *P. icarus* wing scale nanostructure, along with the butterfly wing samples, a series of L-B samples were subjected to  $\text{Al}_2\text{O}_3$  deposition. The Langmuir-Blodgett method is commonly used [40,41] to

prepare photonic crystals from monodisperse sphere layers (usually polymer or silica) deposited in close packing onto flat surfaces in one or more layers. Our experiments resulted in a set of samples with 1, 2, 3, and 5 layers containing only minor irregularities. In the case of multilayers, the presence of additional spheres in lower layers may result in small protrusions on the surface, or vacancy defects may occur, which may affect the optical properties. Examples of such defects on the topmost layer can be seen in Fig. 4(a). In the cross-sectional view of the 5-layer sample, Fig. 4(b), close packing can be seen clearly. Fig. 4(c) shows the ALD coating covering the spheres in a homogeneous and conformal manner in all layers of spheres, narrowing the free space between them [47], which is similar to the closure of the pores observed in the photonic nanoarchitecture of *P. icarus*. The accumulation of deposited material makes the spheres hexagonal (see inset). In such a porous structure there is a certain maximal deposition thickness because

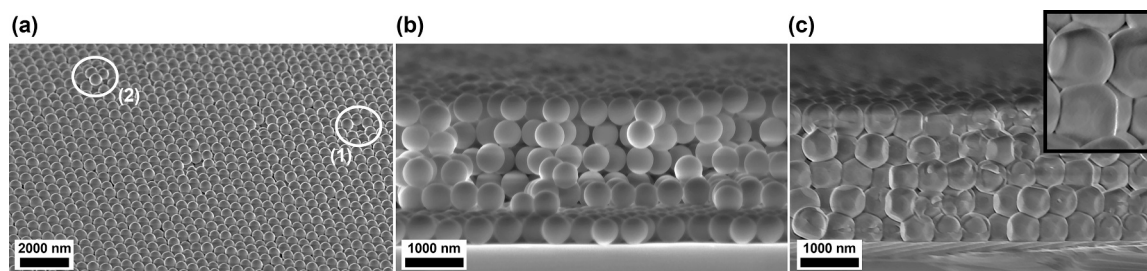


**Fig. 4.** Scanning electron micrographs of a L-B 5-layer sample. (a) Surface view of close-packed hexagonal order with vacancy (1) and additional silica spheres on top (2); (b) cross-sectional view of the as-grown sample; (c) the sample shown in (b) with 40 nm of  $\text{Al}_2\text{O}_3$  added.

complete filling of the voids results in a continuous material (except for the obturated lower pores).

All pristine and ALD-deposited samples with different  $\text{Al}_2\text{O}_3$  layer thicknesses were measured with a goniometric UV-VIS reflectance measurement setup according to the method already described [43] under different incident and reflected angles. Here, an example of optical characterization is presented, performed in a specular,  $40^\circ$  incidence measurement on three samples. The ALD coating shifted the reflectance peaks towards longer wavelengths as the thickness increased (Fig. 5) in accordance with findings reported in Ref. [48]. The color of the as-grown crystal depended on the size of the spheres, which was determined by the synthesis parameters. With the help of ALD, this color was tuned in a controlled way in arbitrary small steps, for layer thicknesses larger than 5 nm (to overstep the growth of separate islands). This can be useful in applications, since, starting from a larger substrate with the same structure, a set of similar and fine-tuned reflectances could easily be obtained.

In order to obtain a numerical relationship between the structural modifications and spectral characteristics of the reflected light, calculations were performed on multilayer models. The simplest case was a thin layer of one material whose thickness decreased during plasma etching. Recently, we demonstrated the origin of *Mimeresia neavei*'s dorsal blue color as a single layer of chitin, the thin adwing lamina of the wing scale [49]. According to TEM data, the thickness of the membrane was measured as  $201 \pm 20$  nm and this chitin–air structure resulted in light reflectance with its main peak at 425 nm. The lamina is the continuous layer of chitin constituting the adwing face of the scale. The schematic structure of a butterfly scale is presented in Fig. 3 of Ref. [3]. The normal incidence reflectance measurement was in accordance with the thin film model calculation. Fig. 3(b) shows the optical effect of structure thinning after a few minutes of plasma treatment for the pepper-pot structure. In the current experiment, the same treatment was used for blue *M. neavei* wing pieces. Normal incidence spectra were recorded on the untreated sample and on the samples after 1, 2, and

3 min of oxygen plasma treatment, as shown in Fig. 6(a). In Fig. 6(b) the calculated spectra on a single thin layer of chitin have their main maxima fitted with the experimental ones. To obtain the specific peak positions, the thickness of the layer in the calculations was decreased from 205 nm (untreated sample, as in [49]) to 145 nm. The correspondence of wavelength minimum and maximum positions is nearly perfect. For intensity differences one has to consider that the real wing-scale contains absorbing pigments, and the wing is formed by a mosaic of partially overlapped ground scales (without structural color) and cover scales (with structural color).

Next, a more complex method, the transfer matrix method [50,51], was used to calculate the reflectance of a structure built of continuous chitin and air layers. This modeled the *P. icarus* wing scales using layers of the same thickness as natural scales measured from TEM images (Fig. 3, and see Ref. [45] for detailed structural analysis). In the pristine state, the scale's nanoarchitecture is built of alternating chitin-rich (refractive index  $\sim 1.56$ ) and air-rich layers (see Fig. 1(i) in Ref [45]) as shown schematically in Fig. 7(a). To model the effect of ALD coating onto the pristine nanoarchitecture, a refractive index of 1.7 was applied with 10–40 nm thickness on both sides of the chitin layer. This is valid because ALD forms a conformal cover layer regardless of depth in these open wing scales – see Fig. 7(a) top. Next, the chitin thickness was decreased (also on both sides) by plasma treatment (Fig. 7(a) bottom). The calculated spectra, Fig. 7(b) and (c), give a good qualitative indication of the nature of the changes obtained during these experiments. Such a simple model of the wing scales cannot reproduce perfectly the measured spectrum because the surface of the butterfly wing shows disorder on several levels [46], and the macroscopically measurable spectrum represents the sum of these effects. In turn the model indicates correctly not only the shift in the reflectance peaks but also the decrease in reflected light intensity with the amount of modification (deposition vs. etching). This is visible on the spectral plots of Fig. 3 and the darker scales in Fig. 1(c), (e), (h), and (j).

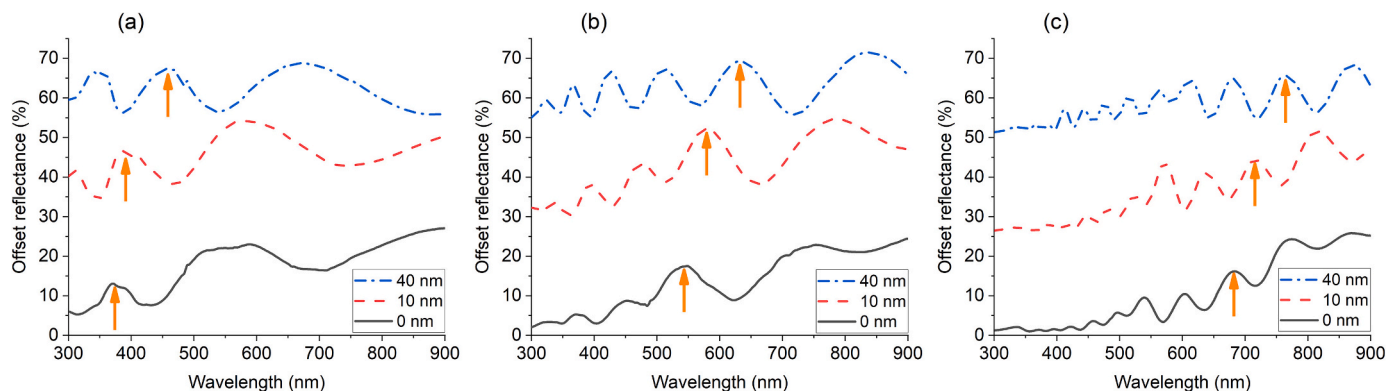


**Fig. 5.** Specular reflectance spectra (offset by 25% for better visibility) of as grown L-B layers, without, with 10 nm and with 40 nm of deposited  $\text{Al}_2\text{O}_3$  L-B samples measured at  $40^\circ$  incident angle. (a) monolayer; (b) bilayer; and (c) 5 layers. The arrows highlight the redshift of the peaks.

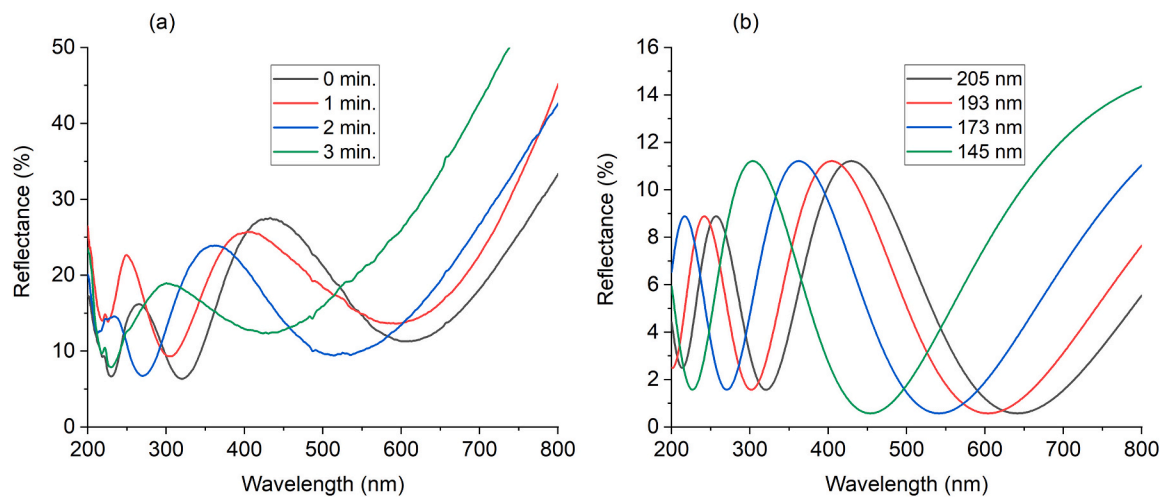


Fig. 6. (a) Normal incidence reflectance spectra of *Mimeresia nevei*'s blue dorsal side, untreated (0 min) and after 1, 2, or 3 min of oxygen plasma treatment. (b) Calculations of single layers to fit the peak position of experimental curves. (For interpretation of the references to color in this figure legend, the reader is referred to the web version of this article.)

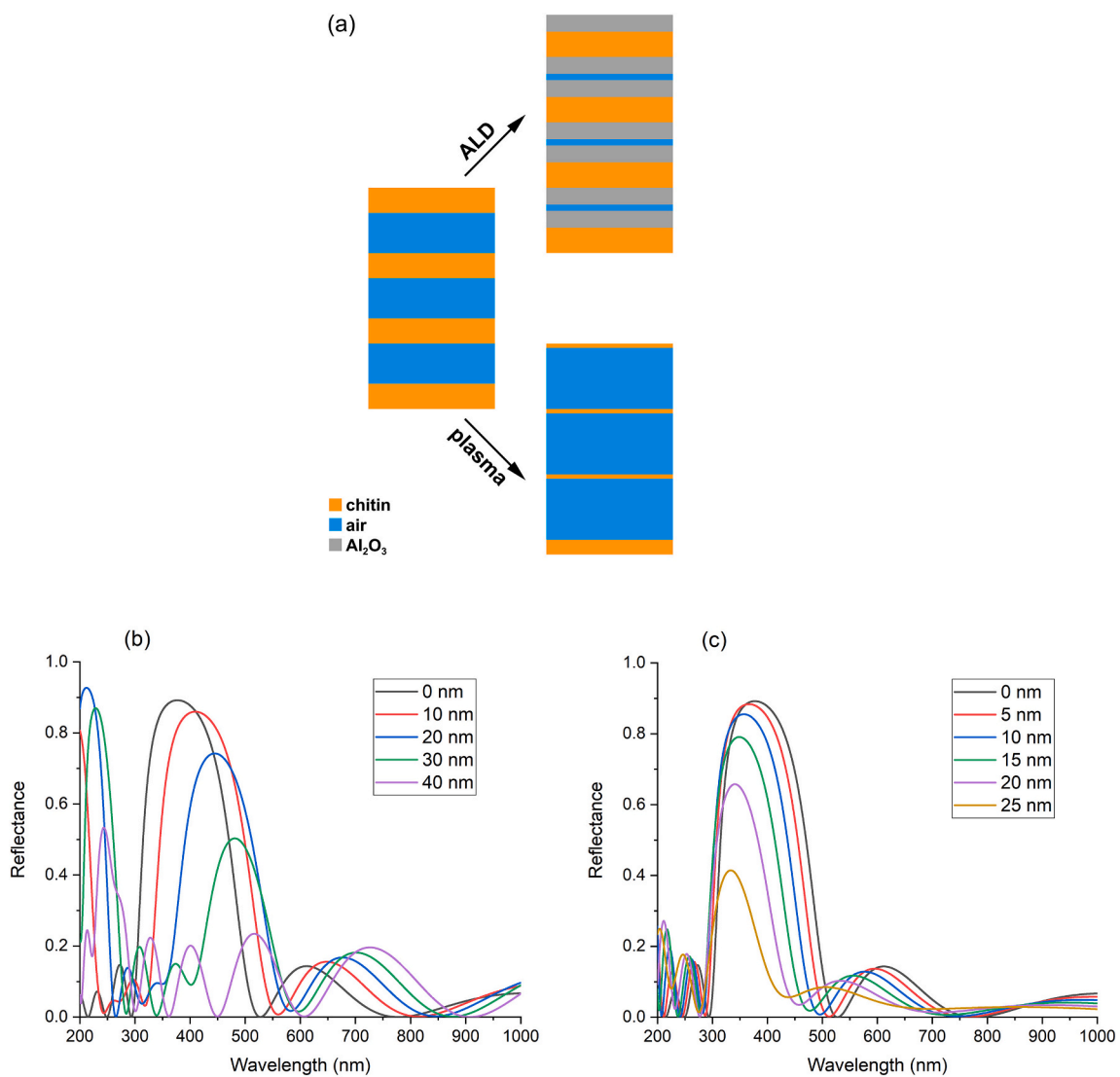


Fig. 7. (a) Multilayer model of *Polyommatus icarus* wing scale: thickening both sides of the chitin layer by Al<sub>2</sub>O<sub>3</sub> addition at the expense of air layers (top); thinning of the chitin by plasma etching (bottom). (b) Calculated normal reflectance spectra on a structure from (a) with deposited Al<sub>2</sub>O<sub>3</sub> layers of 10–40 nm on both sides. (c) The same calculation while thinning the chitin layers by 5–25 nm on both sides.

#### 4. Conclusions

It was demonstrated on butterfly wing scales with open 3D nanostructures that two structural modification methods offer fine and controllable shifting of the reflected light spectrum, one increasing and the other decreasing the reflectance wavelength peaks. The principles and instrumentation of the two methods are completely different, they are complementary in term of spectral modification they produce. In terms of surface chemistry, one builds up the substrate with a conformal, chemically inert coating, and the other removes the original superhydrophobic superficial layer. They open new routes to potential applications.

The overall trends of the spectral modifications observed on butterfly wings were reproduced using both physical and computer models. A physical model, L-B samples of 1, 2, and 5 monolayers, closely matched what had happened on *P. icarus* wings after ALD deposition of a 40 nm Al<sub>2</sub>O<sub>3</sub> layer, namely spectral modifications of 80 nm. For *M. neavei*, the simple thin-film model was found to correctly reproduce the spectral shift of the natural samples. For the more complex pepper-pot structure of *P. icarus* scales, the transfer matrix model was used to calculate the spectral modifications; it predicted spectral shift values similar to those found experimentally, with ca. ±80 nm demonstrated, which means a remarkable ~160 nm of tuning possibility, promising for practical applications.

The experiments with *C. remus* wings demonstrated that the same trends as discussed above for *P. icarus* can be found for other photonic nanoarchitectures: for the photonic single crystal type (blue, dorsal wing side) and for the photonic polycrystal type (green ventral wing side).

#### Funding

This research was supported by the National Research, Development and Innovation Office of Hungary [grant NKFIH K 115724] and [grant NKFIH PD 116579]. The infrastructure for the experimental work was provided by the Hungarian Academy of Sciences.

#### Declaration of Competing Interest

The authors declare that they have no known competing financial interests or personal relationships that could have appeared to influence the work reported in this paper.

#### References

- [1] S.N. Gorb, *Functional Surfaces in Biology: Little Structures With Big Effects 1*, Springer, Netherlands, 2009.
- [2] M. Kolle, S. Lee, Progress and opportunities in soft photonics and biologically inspired optics, *Adv. Mater.* 30 (2018) 1–40, <https://doi.org/10.1002/adma.201702669>.
- [3] L.P. Biró, J.P. Vigneron, Photonic nanoarchitectures in butterflies and beetles: valuable sources for bioinspiration, *Laser Photonics Rev.* 5 (2011) 27–51, <https://doi.org/10.1002/lpor.200900018>.
- [4] K. Yu, T. Fan, S. Lou, D. Zhang, Biomimetic optical materials: integration of nature's design for manipulation of light, *Prog. Mater. Sci.* 58 (2013) 825–873, <https://doi.org/10.1016/j.pmatsci.2013.03.003>.
- [5] D. Zhang, W. Zhang, J. Gu, T. Fan, Q. Liu, H. Su, S. Zhu, Inspiration from butterfly and moth wing scales: characterization, modeling, and fabrication, *Prog. Mater. Sci.* 68 (2015) 67–96, <https://doi.org/10.1016/j.pmatsci.2014.10.003>.
- [6] Z. Han, Z. Mu, W. Yin, W. Li, S. Niu, J. Zhang, L. Ren, Biomimetic multifunctional surfaces inspired from animals, *Adv. Colloid Interf. Sci.* 234 (2016) 27–50, <https://doi.org/10.1016/j.cis.2016.03.004>.
- [7] W. Zhang, J. Gu, Q. Liu, H. Su, T. Fan, D. Zhang, Butterfly effects: novel functional materials inspired from the wings scales, *Phys. Chem. Chem. Phys.* 16 (2014) 19767–19780, <https://doi.org/10.1039/C4CP01513D>.
- [8] Y. Liu, C. Shao, Y. Wang, L. Sun, Y. Zhao, Bio-inspired self-adhesive bright non-iridescent graphene pigments, *Matter* 1 (2019) 1581–1591, <https://doi.org/10.1016/j.matt.2019.08.018>.
- [9] J. Xu, Z. Guo, Biomimetic photonic materials with tunable structural colors, *J. Colloid Interface Sci.* 406 (2013) 1–17, <https://doi.org/10.1016/j.jcis.2013.05.028>.
- [10] Y. Zhao, X. Xie, H. Gu, C. Zhu, Z. Gu, Bio-inspired variable structural color materials, *Chem. Soc. Rev.* 41 (2012) 3297, <https://doi.org/10.1039/c2cs15267c>.
- [11] Z. Chen, F. Fu, Y. Yu, H. Wang, Y. Shang, Y. Zhao, Cardiomyocytes-actuated morpho butterfly wings, *Adv. Mater.* 31 (1–7) (2019), <https://doi.org/10.1002/adma.201805431>.
- [12] F. Fu, L. Shang, Z. Chen, Y. Yu, Y. Zhao, Bioinspired living structural color hydrogels, *Sci. Robot.* 3 (2018), <https://doi.org/10.1126/SCIROBOTICS.AAR8580>.
- [13] H. Wang, Y. Liu, Z. Chen, L. Sun, Y. Zhao, Anisotropic structural color particles from colloidal phase separation, *Sci. Adv.* 6 (2020), <https://doi.org/10.1126/sciadv.aay1438>.
- [14] Q. Yang, S. Zhu, W. Peng, C. Yin, W. Wang, J. Gu, W. Zhang, J. Ma, T. Deng, C. Feng, D. Zhang, Bioinspired fabrication of hierarchically structured, pH-tunable photonic crystals with unique transition, *ACS Nano* 7 (2013) 4911–4918, <https://doi.org/10.1021/nn400090j>.
- [15] R. Potyrailo, R.R. Naik, Bionanomaterials and bioinspired nanostructures for selective vapor sensing, *Annu. Rev. Mater. Res.* 43 (43) (2013) 307–334, <https://doi.org/10.1146/annurev-matsci-071312-121710>.
- [16] G. Piszter, K. Kertész, Z. Vértessy, Z. Bálint, L.P. Biró, Substance specific chemical sensing with pristine and modified photonic nanoarchitectures occurring in blue butterfly wing scales, *Opt. Express* 22 (2014) 22649–22660, <https://doi.org/10.1364/OE.22.022649>.
- [17] Z. Luo, Z. Weng, Q. Shen, S. An, J. He, B. Fu, R. Zhang, P. Tao, C. Song, J. Wu, T. Deng, W. Shang, Vapor detection through dynamic process of molecule desorption from butterfly wings, *Pure Appl. Chem.* (2019), <https://doi.org/10.1515/pac-2019-0118>.
- [18] Y. Tan, J. Gu, W. Xu, Z. Chen, D. Liu, Q. Liu, D. Zhang, Reduction of CuO butterfly wing scales generates Cu SERS substrates for DNA base detection, *ACS Appl. Mater. Interfaces* 5 (2013) 9878–9882, <https://doi.org/10.1021/am402699c>.
- [19] Y. Tan, J. Gu, L. Xu, X. Zang, D. Liu, W. Zhang, Q. Liu, S. Zhu, H. Su, C. Feng, G. Fan, D. Zhang, High-density hotspots engineered by naturally piled-up subwavelength structures in three-dimensional copper butterfly wing scales for surface-enhanced Raman scattering detection, *Adv. Funct. Mater.* 22 (2012) 1578–1585, <https://doi.org/10.1002/adfm.201102948>.
- [20] R.E. Rodríguez, S.P. Agarwal, S. An, E. Kazyak, D. Das, W. Shang, R. Skye, T. Deng, N.P. Dasgupta, Biotemplated *Morpho* butterfly wings for tunable structurally colored photocatalysts, *ACS Appl. Mater. Interfaces* 10 (2018) 4614–4621, <https://doi.org/10.1021/acsami.7b14383>.
- [21] T. Wagner, C. Neinhuis, W. Barthlott, Wettability and contaminability of insect wings as a function of their surface sculptures, *Acta Zool.* 77 (1996) 213–225, <https://doi.org/10.1111/j.1463-6395.1996.tb01265.x>.
- [22] D. Byun, J. Hong, J.H. Saputra, Y.J. Ko, H.C. Lee, B.K. Park, J.R. Lukes Byun, Wetting characteristics of insect wing surfaces, *J. Bionic Eng.* 6 (2009) 63–70, [https://doi.org/10.1016/S1672-6529\(08\)60092-X](https://doi.org/10.1016/S1672-6529(08)60092-X).
- [23] Y. Ding, S. Xu, Y. Zhang, A.C. Wang, M.H. Wang, Y. Xiu, C.P. Wong, Z.L. Wang, Modifying the anti-wetting property of butterfly wings and water strider legs by atomic layer deposition coating: surface materials versus geometry, *Nanotechnology* 19 (2008), 355708, <https://doi.org/10.1088/0957-4484/19/35/355708>.
- [24] S.M. George, Atomic layer deposition: an overview, *Chem. Rev.* 110 (2010) 111, <https://doi.org/10.1021/cr900056b>.
- [25] T. Nam, H. Kim, Atomic layer deposition for nonconventional nanomaterials and their applications, *J. Mater. Res.* 35 (2020) 656–680, <https://doi.org/10.1557/jmr.2019.347>.
- [26] J.A. Noyes, P. Vukusic, I.R. Hooper, Experimental method for reliably establishing the refractive index of buprestid beetle exocuticle, *Opt. Express* 15 (2007) 4351, <https://doi.org/10.1364/oe.15.004351>.
- [27] A.R. Parker, D.R. McKenzie, M.C.J. Large, Multilayer reflectors in animals using green and gold beetles as contrasting examples, *J. Exp. Biol.* 201 (1998) 1307–1313.
- [28] K. Kertész, G. Molnár, Z. Vértessy, A.A. Koós, Z.E. Horváth, G.I. Márk, L. Tapasztó, Zs Bálint, I. Tamáska, O. Deparis, J.P. Vigneron, L.P. Biró, Photonic band gap materials in butterfly scales: A possible source of “blueprints”, *Mater. Sci. Eng. B* 149 (2008) 259–265, <https://doi.org/10.1016/j.mseb.2007.10.013>.
- [29] K. Michielsen, D.G. Stavenga, Gyroid cuticular structures in butterfly wing scales: biological photonic crystals, *J. R. Soc. Interface* 5 (2008) 85–94, <https://doi.org/10.1098/rsif.2007.1065>.
- [30] B.D. Wilts, X. Sheng, M. Holler, A. Diaz, M. Guizar-Sicairos, J. Raabe, R. Hoppe, S. H. Liu, R. Langford, O.D. Onelli, D. Chen, S. Torquato, U. Steiner, C.G. Schroer, S. Vignolini, A. Sepe, Evolutionary-optimized photonic network structure in white beetle wing scales, *Adv. Mater.* 30 (2018) 1–6, <https://doi.org/10.1002/adma.201702057>.
- [31] S. Berthier, *Photonique des Morphos*, Springer, 2010.
- [32] M.A. Giraldo, S.S. Yoshioka, C. Liu, D.G. Stavenga, Coloration mechanisms and phylogeny of *Morpho* butterflies, *J. Exp. Biol.* 219 (2016) 3936–3944, <https://doi.org/10.1242/jeb.148726>.
- [33] J.Y. Huang, X.D. Wang, Z.L. Wang, Controlled replication of butterfly wings for achieving tunable photonic properties, *Nano Lett.* 6 (2006) 2325–2331, <https://doi.org/10.1021/nl061851t>.
- [34] Y. Liu, L. Huang, W. Shi, Structural color bio-engineering by replicating *Morpho* wings, *Adv. Mater. Res.* 391–392 (2012) 409–417, <https://doi.org/10.4028/www.scientific.net/AMR.391-392.409>.
- [35] F. Liu, W. Shi, X. Hu, B. Dong, Hybrid structures and optical effects in *Morpho* scales with thin and thick coatings using an atomic layer deposition method, *Opt. Commun.* 291 (2013) 416–423, <https://doi.org/10.1016/j.optcom.2012.11.034>.
- [36] F. Liu, Y. Liu, L. Huang, X. Hu, B. Dong, W. Shi, Y. Xie, X. Ye, Replication of homologous optical and hydrophobic features by templating wings of butterflies *Morpho menelaus*, *Opt. Commun.* 284 (2011) 2376–2381, <https://doi.org/10.1016/j.optcom.2011.01.017>.

- [37] D.P. Gaillot, O. Deparis, V. Welch, B.K. Wagner, J.P. Vigneron, C.J. Summers, Composite organic-inorganic butterfly scales: production of photonic structures with atomic layer deposition, *Phys. Rev. E* 78 (2008) 031922, <https://doi.org/10.1103/PhysRevE.78.031922>.
- [38] C.J. Summers, D.P. Gaillot, M. Crne, J. Blair, J.O. Park, M. Srinivasarao, O. Deparis, V. Welch, J.P. Vigneron, Investigations and mimicry of the optical properties of butterfly wings, *J. Nonlinear Opt. Phys. Mater.* 19 (2010) 489–501, <https://doi.org/10.1142/S0218863510005339>.
- [39] Q. Shen, J. He, M. Ni, C. Song, L. Zhou, H. Hu, R. Zhang, Z. Luo, G. Wang, P. Tao, T. Deng, W.S. Shang, Subtractive structural modification of *Morpho* butterfly wings, *Small* 11 (2015) 5705–5711, <https://doi.org/10.1002/sml.201500502>.
- [40] S. Portal-Marco, M.À. Vallvé, O. Arteaga, J. Ignés-Mullol, C. Corbella, E. Bertran, Structure and physical properties of colloidal crystals made of silica particles, *Coll. Surf. A Physicochem. Eng. Asp.* 401 (2012) 38–47, <https://doi.org/10.1016/j.colsurfa.2012.03.007>.
- [41] S. Reclusa, S. Ravaine, Colloidal photonic crystals obtained by the Langmuir–Blodgett technique, *Appl. Surf. Sci.* 246 (2005) 409–414, <https://doi.org/10.1016/j.apsusc.2004.11.066>.
- [42] A. Deák, I. Székely, E. Kálmán, Zs. Keresztes, A.L. Kovács, Z. Hörvölgyi, Nanostructured silica Langmuir–Blodgett films with antireflective properties prepared on glass substrates, *Thin Solid Films* 484 (2005) 310–317, <https://doi.org/10.1016/j.tsf.2005.01.096>.
- [43] K. Kertész, Zs. Bálint, Z. Vértsey, G.I. Márk, V. Lousse, J.P. Vigneron, M. Rassart, L. P. Biró, Gleaming and dull surface textures from photonic-crystal-type nanostructures in the butterfly *Cyanophrys remus*, *Phys. Rev. E Stat. Nonlinear Soft Matter. Phys.* 74 (2006) 21922, <https://doi.org/10.1103/PhysRevE.74.021922>.
- [44] B.D. Wilts, B.A. Zubiri, M.A. Klatt, B. Butz, M.G. Fischer, S.T. Kelly, E. Spiecker, U. Steiner, G.E. Schröder-Turk, Butterfly gyroid nanostructures as a time-frozen glimpse of intracellular membrane development, *Sci. Adv.* 3 (2017) 1–8, <https://doi.org/10.1126/sciadv.1603119>.
- [45] Z. Bálint, K. Kertész, G. Piszter, Z. Vértsey, L.P. Biró, The well-tuned blues: the role of structural colours as optical signals in the species recognition of a local butterfly fauna (Lepidoptera: Lycaenidae: Polyommatainae), *J. R. Soc. Interface* 9 (2012) 1745–1756, <https://doi.org/10.1098/rsif.2011.0854>.
- [46] G. Piszter, K. Kertész, Z. Bálint, L.P. Biró, Variability of the structural coloration in two butterfly species with different prezygotic mating strategies, *PLoS One* 11 (2016) 1–19, <https://doi.org/10.1371/journal.pone.0165857>.
- [47] J.S. King, D. Heineman, E. Graugnard, C.J. Summers, Atomic layer deposition in porous structures: 3D photonic crystals, *Appl. Surf. Sci.* 244 (2005) 511–516, <https://doi.org/10.1016/j.apsusc.2004.10.110>.
- [48] Z.A. Sechrist, B.T. Schwartz, J.H. Lee, J.A. McCormick, R. Piestun, W. Park, S. M. George, Modification of opal photonic crystals using Al<sub>2</sub>O<sub>3</sub> atomic layer deposition, *Chem. Mater.* 18 (2006) 3562–3570, <https://doi.org/10.1021/cm060263d>.
- [49] Z. Bálint, S. Sáfián, A. Hoskins, K. Kertész, A.A. Koós, Z.E. Horváth, G. Piszter, L. P. Biró, The only blue *Mimeresia* (Lepidoptera: Lycaenidae: Lipteninae) uses a color-generating mechanism widely applied by butterflies, *J. Insect Sci.* 18 (1–8) (2018), <https://doi.org/10.1093/jisesa/iey046>.
- [50] J.B. Pendry, A. MacKinnon, Calculation of photon dispersion relations, *Phys. Rev. Lett.* 69 (1992) 2772–2775, <https://doi.org/10.1103/PhysRevLett.69.2772>.
- [51] P. Yeh, *Optical Waves in Layered Media*, Wiley, New York, 2005.